Time-resolved fluorescence and computational studies of adenylylated glutamine synthetase: Analysis of intersubunit interactions

ARTICLE *in* PROTEIN SCIENCE · MAY 1993

Impact Factor: 2.85 · DOI: 10.1002/pro.5560020510 · Source: PubMed

4 AUTHORS, INCLUDING:

William M Atkins
University of Washington Seattle
135 PUBLICATIONS **3,249** CITATIONS

SEE PROFILE

Protein Science (1993), *2*, 800–813. Cambridge University Press. Printed in the USA.

Time-resolved fluorescence and computational studies of adenylylated glutamine synthetase: Analysis of intersubunit interactions

WILLIAM M. ATKINS,[1] BETH M. CADER,[2] JENS HEMMINGSEN,[2,3] AND JOSEPH J. VILLAFRANCA[2]

[1] Department of Medicinal Chemistry, University of Washington, Seattle, Washington 98195
[2] Department of Chemistry, The Pennsylvania State University, University Park, Pennsylvania 16802

(RECEIVED November 24, 1992; REVISED MANUSCRIPT RECEIVED January 21, 1993)

Abstract

Adenylylation of Tyr-397 of each subunit of *Escherichia coli* glutamine synthetase (GS) down-regulates enzymatic activity in vivo. The overall structure of the enzyme consists of 12 subunits arranged as two hexamers, face to face. Research reported in this paper addresses the question of whether the covalently attached adenylyl group interacts with neighboring amino acid residues to produce the regulatory phenomenon. Wild-type GS has two Trp residues (positions 57 and 158) and the adenylylation site lies within 7–8 Å of the Trp-57 loop in the adjacent subunit of the same hexameric ring; Trp-158 is about 35 Å from the site of adenylylation. Fluorescence lifetimes and quantum yields have been determined for two fluorophores with wild-type and mutant GS. One fluorophore is ε-AMP adenylylated GS (at Tyr-397), and the other fluorophore is the intrinsic protein residue Trp-57. These experiments were conducted in order to detect possible intersubunit interactions between adenylyl groups and the neighboring Trp-57 to search for a role for the Trp-57 loop in the regulation of GS. The fluorescence due to ε-AMP of two adenylylated enzymes, wild-type GS and the W158F mutant, exhibits heterogeneous decay kinetics; the data adequately fit to a double exponential decay model with recovered average lifetime values of 18.2 and 2.1 ns, respectively. The pre-exponential factors range from 0.66 to 0.73 for the long lifetime component, at five emission wavelengths. The W57L-ε-AMP enzyme yields longer average lifetime values of 19.5 and 2.4 ns, and the pre-exponential factors range from 0.82 to 0.85 for the long lifetime component. An additional residue in the Trp-57 loop, Lys-58, has been altered and the K58C mutant enzyme has been adenylylated with ε-AMP on Tyr-397. Lys-58 is near the ATP binding site and may represent a link by which the adenylyl group controls the activity of GS. The fluorescence of ε-AMP-adenylylated K58C mutant GS is best described by a triple exponential decay with average recovered lifetime values of 19.9, 4.6, and 0.58 ns, with the largest fraction being the median lifetime component. Relative quantum yields of ε-AMP–Tyr-397 were measured in order to determine if static quenching occurs from adenine–indole stacking in the wild-type GS. The relative quantum yield of the ε-AMP-adenylylated W57L mutant is larger than the wild-type protein by the amount predicted from the difference in lifetime values: thus, no static quenching is evident. Intrinsic tryptophan fluorescence was also studied in the presence and absence of covalently attached adenylyl groups. The fluorescence decay parameters of Trp-57 are not significantly affected by the presence of ε-AMP or AMP attached to Tyr-397. Enzymatic activity of the mutant proteins was also studied. The Mg-activated enzymes are nearly completely inhibited upon adenylylation, and regulation is not affected by mutation at Trp-57 or Lys-58. These results indicate that the Trp-57 loop dynamically interacts with the adenylyl group, but a "ring stacked" complex is not formed and is not a structural feature of the regulatory mechanism. This conclusion was further corroborated by computational minimization and molecular dynamics studies of GS with an AMP moiety built onto Tyr-397. Relative energies were sampled at various points as the Trp-57 ring and purine ring of AMP were targeted toward one another, the endpoint being a 3-Å parallel and

[3] Present address: Department of Biochemistry, Duke University, Durham, North Carolina 27710.

Reprint requests to: Joseph J. Villafranca, Pharmaceutical Research Institute, Bristol-Myers Squibb, P.O. Box 4000, Princeton, New Jersey 08540-4000.

Abbreviations: GS, glutamine synthetase; ATP, adenosine-5′-triphosphate; AMP, adenosine-5′-monophosphate; ε-AMP, 1,N^6-ethenoadenosine-5′-monophosphate; DAS, decay-associated spectra; TRES, time-resolved emission spectrum; W158F, the site-directed mutant in which tryptophan 158 is replaced by phenylalanine; W57L, the site-directed mutant in which tryptophan 57 is replaced by leucine; K58C, the site-directed mutant in which lysine 58 is replaced by cysteine; ind-C_3-ade, 3-(indol-1-yl)propyladenine; ATase, adenylyltransferase.

stacked conformation. Dynamics simulations were performed with the parallel, stacked conformation, as well as an extended conformation, as the starting point. All studies indicate that the stacked indole–purine conformation is not favorable; however, a potential hydrogen bonding interaction between the amine nitrogen of the tryptophan and the ring oxygen of ribose is implied by dynamics simulations for certain conformations of the loop.

Keywords: ε-AMP; conformation; enzyme activity; molecular dynamics; mutants

The use of intrinsic protein fluorescence as a probe of protein structure and dynamics has increased dramatically as a result of advances in instrumentation; likewise, these advances in analytical methods allow for accurate determination of decay kinetics of complex mixtures of fluorophores (Beechem et al., 1983; Jameson et al., 1984; Alcala et al., 1987). The increase in sophistication of the interpretation of time-resolved fluorescence data has been aided by genetic engineering methods that allow for the placement of a unique tryptophan or tyrosine residue at defined locations within a protein structure. The utility of fluorescence methodologies would be greatly enhanced if additional fluorophores, other than the naturally occurring amino acids, could be attached at specified locations on proteins. The ε family of nucleotide analogues has provided valuable steady-state fluorescent probes of many nucleotide-binding proteins (Secrist et al., 1972), including glutamine synthetase (Chock et al., 1973; Villafranca et al., 1978). Here we report fluorescence lifetime measurements with *Escherichia coli* GS and site-directed mutants adenylylated with ε-AMP at the physiological site of adenylylation, Tyr-397.

GS catalyzes the reaction of ATP with glutamate and ammonia to afford glutamine, ADP, and P_i. GS from several bacterial sources is regulated by covalent modification, where a specific tyrosine is adenylylated by the enzyme ATase (Shapiro et al., 1967). This residue is Tyr-397 for *E. coli* GS. The X-ray crystal structure of the nearly identical *Salmonella typhimurium* GS indicates that Tyr-397 lies at the outer diameter of the hexagonal ring structure formed from six identical subunits. Two of these hexagonal rings are joined face to face to afford a dodecameric GS in bacteria. As a result of adenylylation at Tyr-397, the Mn-enzyme and the Mg-enzyme exhibit a 4-fold and 37-fold increase in the K_m for ATP, respectively (Abell & Villafranca, 1991). Furthermore, fluorescence experiments have indicated that a conformational change occurs within the Trp-57 loop when ATP binds (Atkins et al., 1991), and the magnitude of this conformational change is greatly reduced in the adenylylated Mg-enzyme (Rhee et al., 1982). Therefore, it is possible that the adenylyl group attached to Tyr-397 serves to decrease the affinity of the enzyme for ATP by preventing a substrate-induced conformational change.

Tyr-397 on one subunit within the dodecamer lies within 8 Å of the Trp-57 loop in the adjacent subunit (Kinemage 1). It has been proposed that interactions between the adenylyl group and the Trp-57 loop are important in the regulation of GS activity (Almassy et al., 1986). Specific "stacking" interaction between the adenylyl purine ring and the indole of Trp-57 is easily imagined as a means for communication between the regulatory group and the active site, since the Trp-57 loop connects two β-strands that cross the active site (Fig. 1). It is also possible that two adenylyl groups on adjacent hexameric rings might interact to prevent the protein from undergoing conformational changes necessary for catalysis. (Indole)–(purine) and (purine)–(purine) stacking interactions

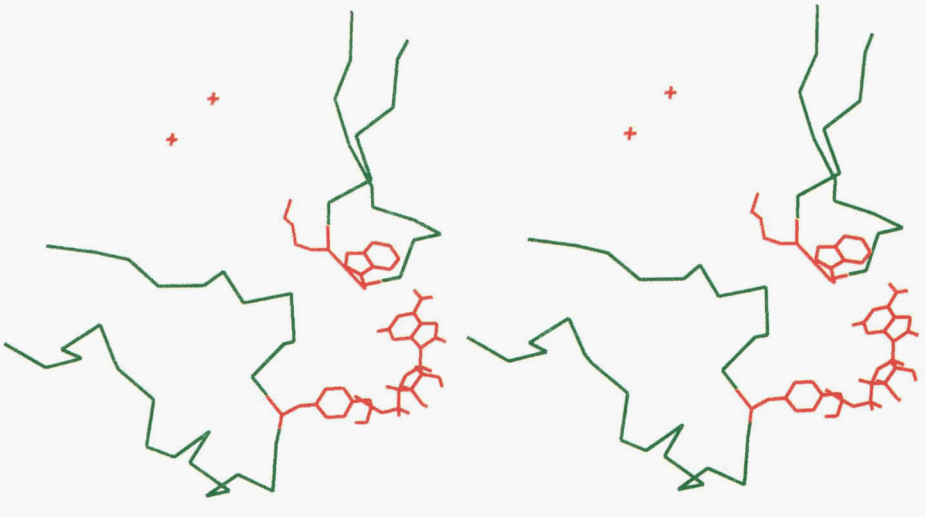

Fig. 1. Stereo view showing the minimized α-carbon trace (green) of the Tyr-397 and Trp-57 loops used in the computer modeling studies. Trp-57 and Lys-58, as well as adenylylated Tyr-397 from the adjacent subunit, are in red. The two pluses (+) represent the nearest boundary of the active site defined by these adjacent subunits; the distance from the active site to Trp-57 is approx. 23 Å.

have been studied extensively with model compounds and in proteins (Tolman et al., 1974; Gruber & Leonard, 1975; Mutai et al., 1975; Liou & Anderson, 1978). It has been shown that when "caged," fluorescent nucleotides, which have a $1,N^6$-etheno bridge, are complexed with indoles or tryptophan, their fluorescent properties are changed. Specifically, ε-AMP and congeners are dynamically and statically quenched in model compounds where the indole and purine are in equilibrium between "complexed" and "open" forms. The "complexed" form has purine and indole rings stacked, contacting in a parallel arrangement. The stacked form does *not* exhibit unique fluorescent properties, such as a red-shifted excimer. The major effect that indole stacking has on ε-purine fluorescence is static quenching that results in a "dark" (indole)–(purine) complex with vanishingly small quantum yield. In intramolecular (ε-purine)–(indole) complexes, the fraction of complexes in the "dark," stacked complex and in the "open" complex can be determined by measurement of the fluorescence lifetime and the quantum yield of the ε-purine (Gruber & Leonard, 1975; Mutai et al., 1975). This model chemistry has prompted the use of ε-adenylyl GS as a fluorescent probe of intramolecular (Trp-57)–(adenylyl) interactions in GS. Additional insight into these interactions is given by computational minimization and molecular dynamics studies.

Results

Steady-state fluorescence

The steady-state fluorescent properties of ε-adenylylated GS have been described previously (Chock et al., 1973; Villafranca et al., 1978). With an excitation wavelength of 310 nm, the ε-adenylylated protein has a broad emission spectrum with an emission maximum at 412 nm. The emission spectra of the wild-type protein, the W158F mutant, and the W57L mutant are essentially identical. In all three protein spectra, there is a small shoulder on the blue side at approximately 385 nm. This observation is noteworthy in light of the temperature and viscosity dependence observed for the emission maximum by Secrist et al. (1972), where it is demonstrated that such a blue shift reflects constraints on molecular motion within the nucleotide. It is also noteworthy that the emission maximum of the ε-adenylylated GS is blue-shifted 4–5 nm from the emission maximum of the free ε-ATP at 417 nm.

Fluorescence lifetime measurements

Fluorescence lifetimes were determined at 380, 410, 440, 470, and 500 nm. Fluorescence lifetime measurements with free ε-ATP demonstrated that the fluorescence decay kinetics reflect a single, homogeneous exponential decay with an average lifetime value of 21.4 ns, as previously demonstrated (Secrist et al., 1972). The fluorescence lifetime of the free probe was constant over several wavelengths spanning the emission spectrum. Attempts to fit the decay data to a sum of two or three exponentials resulted in recovery of identical lifetime values for the individual components. A typical decay profile is shown in Figure 2.

In contrast, when the wild-type enzyme is adenylylated with ε-ATP, the decay data are best fit to a sum of two exponential decays. The recovered lifetime values are 17.9–18.5 ns and 1.9–2.4 ns. The pre-exponential factors, when combined with the lifetime values, indicate that nearly all (92–94%) of the fractional intensity of emission is from the longer lifetime component (Table 1). Single exponential fits of the data yielded χ^2 values of 5 or greater, whereas fitting the data to the sum of two exponentials afforded χ^2 values of 1.6 or lower, for individual wavelengths. With more complex models, using the sum of three exponentials, the χ^2 values did not improve significantly, so it is clear that the ε-adenylyl group on the protein is best described by a sum of two exponential decay processes. Such heterogeneous decay kinetics have been shown for many single-tryptophan-containing proteins (Hutnik & Szabo, 1989a; Royer et al., 1990; Atkins et al., 1991). It should be pointed out that the differences in fluorescence decay of the free ε-ATP and ε-AMP

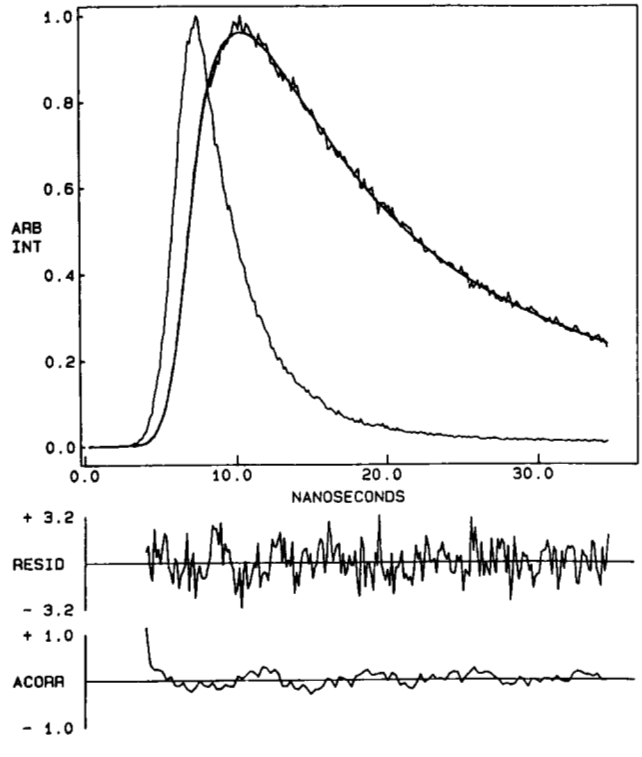

Fig. 2. Fluorescence decay profile of free ε-ATP. The fluorescence decay of the free ε-ATP in 50 mM Hepes, pH 7.4, 100 mM KCl, 25 mM $MgCl_2$ is shown, along with the lamp decay profile. The smooth curve drawn through the decay data is the best single exponential fit. The weighted residuals and autocorrelation are also shown.

Table 1. *Fluorescence parameters for ε-ATP and adenylylated proteins*[a]

Protein	Best exponential model	τ (ns), α at wavelength				
		380 nm	410 nm	440 nm	470 nm	500 nm
Free ε-ATP	Single	22.4, 1.0 $\chi^2 = 1.42$	21.6, 1.0 $\chi^2 = 1.05$	21.3, 1.0 $\chi^2 = 1.19$	21.2, 1.0 $\chi^2 = 1.17$	
Wild type	Double	17.7, 0.68 2.1, 0.32 $\chi^2 = 1.68$	18.2, 0.72 2.1, 0.28 $\chi^2 = 2.26$	18.5, 0.73 2.1, 0.27 $\chi^2 = 2.38$	18.1, 0.70 1.9, 0.27 $\chi^2 = 2.35$	18.0, 0.7 2.4, 0.30 $\chi^2 = 2.09$
W158F	Double	17.7, 0.66 2.2, 0.34 $\chi^2 = 1.56$	18.3, 0.71 2.3, 0.29 $\chi^2 = 1.71$	18.5, 0.74 2.3, 0.26 $\chi^2 = 1.72$	18.8, 0.70 1.9, 0.30 $\chi^2 = 1.57$	18.9, 0.70 1.9, 0.30 $\chi^2 = 1.87$
W57L	Double	19.3, 0.82 2.5, 0.18 $\chi^2 = 1.69$	19.3, 0.85 2.3, 0.15 $\chi^2 = 1.64$	19.7, 0.84 2.5, 0.16 $\chi^2 = 1.65$	19.8, 0.82 2.4, 0.18 $\chi^2 = 1.59$	19.8, 0.82 2.4, 0.18 $\chi^2 = 1.36$
K58C	Triple		19.9, 0.19 4.8, 0.21 0.64, 0.60 $\chi^2 = 1.86$	19.9, 0.19 4.4, 0.25 0.52, 0.57 $\chi^2 = 1.40$		

[a] Excitation was at 310 nm. The excited state lifetimes of each component, τ, are followed by the pre-exponential factors, α. The standard deviations (not shown) for the individual lifetime values are ±0.04 or less for each wavelength. χ^2 values are calculated according to standard least-squares analysis as $\sum \omega_i [R(t) - R_c(t)]^2$, where ω_i is a statistical weighting factor provided in the instrumental software. Measurements were performed with 20 μM glutamine synthetase in 50 mM Hepes, pH 7.5, 100 mM KCl, 25 mM $MgCl_2$.

attached to Tyr-397 are not a result of the loss of two phosphoryl linkages. ε-AMP in solution also exhibits homogeneous decay, with a lifetime of 22 ns under the conditions used here (Spencer et al., 1974). It is clear that protein residues near the adenylyl group produce dynamic quenching. It is striking that there is very little wavelength dependence of the recovered lifetime values. This is evident from the TRES shown in Figure 3, where no shift in the emission maximum is evident as the decay progresses.

The ability to specifically adenylylate Tyr-397 with ε-AMP on site-directed mutants of GS provides a probe of possible interactions between the adenylylation site and the Trp-57 loop. The W57L mutant has been adenylylated and the fluorescence lifetimes of the nucleotide have been determined. In addition, the W158F mutant has been adenylylated and analyzed in the same manner. Although Trp-158 is on the opposite side of the protein, approximately 20 Å from Tyr-397, it was necessary to determine if any changes in tryptophan fluorescence or ε-adenylyl fluorescence observed in the W57L mutant could be directly attributed to Trp-57. W158F provides a negative experimental control for structural or optical changes caused by mutation of the Trp-57 loop.

When the fluorescence decay of the ε-AMP-adenylylated W158F mutant is analyzed, it is clear that it also is best fit to the sum of two exponential decays, with recovered lifetime values that are essentially identical to those of the wild-type enzyme (Table 1). The single and double exponential decay models for the W158F mutant are com-

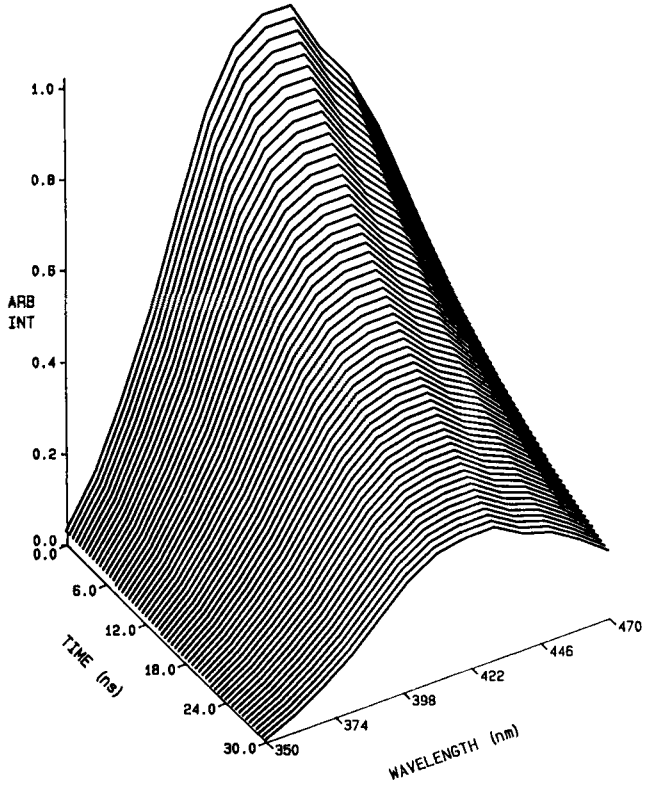

Fig. 3. Time-resolved emission spectrum (TRES) of ε-AMP-adenylylated glutamine synthetase (GS). The TRES of the ε-AMP indicates no significant time dependence of the emission spectrum. Excitation was at 310 nm. The spectrum was constructed using decay data obtained at five emission wavelengths.

pared in Figure 4. The average lifetime values are 18.4 and 2.2 ns, with nearly identical pre-exponential factors at each wavelength. As with the wild-type protein, there is no significant wavelength dependence of the lifetime values or the fractional intensities. Therefore, it is clear that mutation at a Trp residue far from the site of adenylylation has no effect on the fluorescence decay properties of the bound ε-adenylyl group.

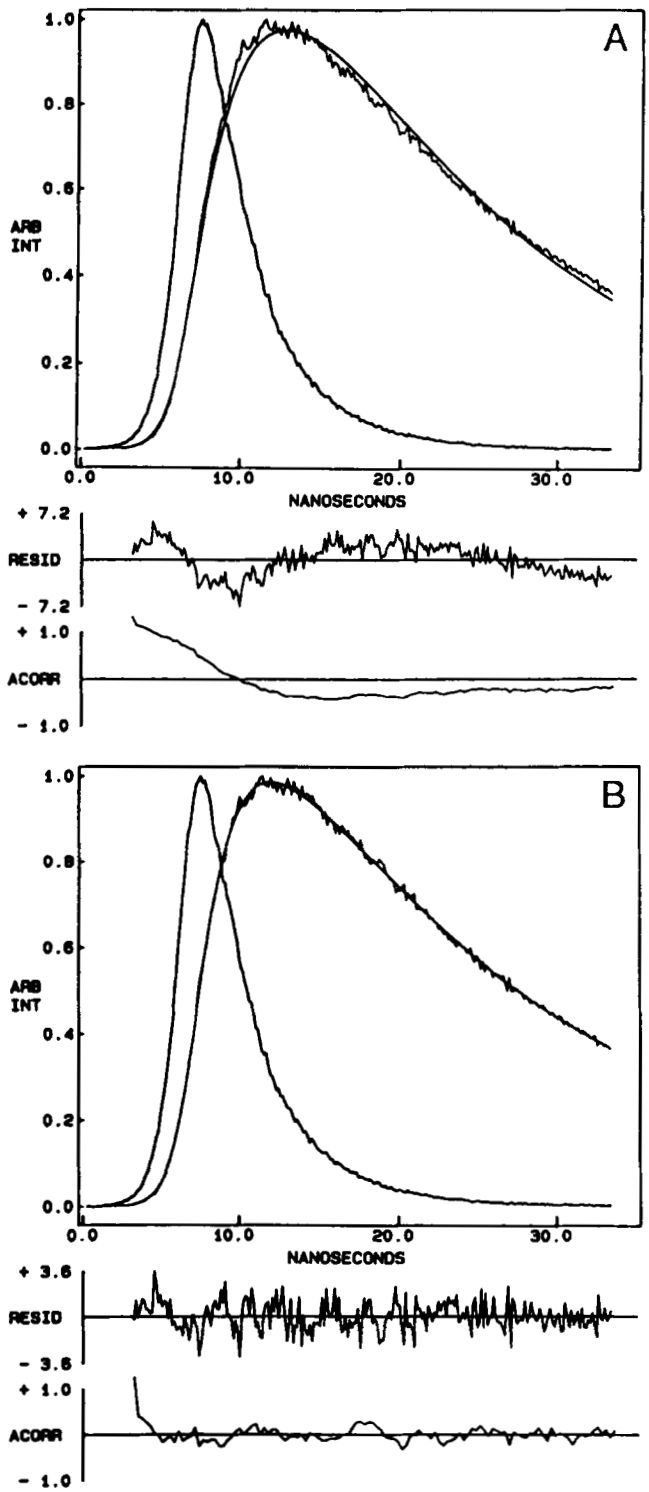

Fig. 4. Comparison of single and double exponential models for ε-AMP bound to W158F. **A:** Single exponential model. **B:** Double exponential model.

When the W57L mutant is adenylylated with ε-AMP and analyzed in a similar way a small, reproducible difference is observed in the recovered lifetimes and pre-exponential values. Like the wild-type and W158F proteins, ε-AMP bound to W57L exhibits heterogeneous decay that fits adequately to a double exponential decay. At each of the wavelengths spanning the emission spectrum, the recovered lifetime values are slightly longer and the pre-exponential factors are shifted to favor the longer lifetime, that is, the fluorescence of the ε-adenylyl group on the W57L mutant decays more slowly than on the wild-type protein. Although this difference in the recovered lifetime values between the W57L mutant and the wild-type and W158F proteins is small, it has been reproducibly observed with several preparations of adenylylated enzymes. Furthermore, multifrequency phase/modulation experiments demonstrate similar results, in which the frequency response of the ε-adenylyl W57L mutant is slightly shifted toward lower frequencies compared to the wild-type and W158F proteins (data not shown). The lifetime values recovered from the phase and modulation data at emission wavelengths of 410 and 440 nm are longer for the W57L mutant than for the wild-type protein and show the same trend toward a larger proportion of the longer lifetime component, as observed with the time domain experiments.

In order to determine whether specific structural features of the Trp-57 loop are correlated to this observed difference in the fluorescence decay parameters of the ε-adenylyl group, an additional mutant protein was adenylylated with ε-AMP. Lys-58, next to Trp-57, is considered to be involved in binding of ATP and phosphorylated intermediates formed during catalysis by GS. It is highly conserved among several bacterial GSs (Wray & Lewis, 1988; Pesole et al., 1991) and may provide part of a consensus nucleotide-binding loop (Wierenga et al., 1986). The fluorescence decay kinetics of the ε-adenylyl K58C mutant were determined at only two wavelengths: 410 and 440 nm. This mutant enzyme was a poor substrate for the enzymatic adenylylation reaction catalyzed by ATase, so samples of ε-AMP-K58C were not fully adenylylated. Therefore, lifetime measurements were only performed at wavelengths near the emission maximum, 410 and 440 nm, due to decreased sensitivity. The decay kinetics are clearly different from the wild-type and W158F proteins. The K58C mutant is best described by a triple exponential decay. A model using the sum of two exponentials yields χ^2 values of 2.4–2.6. Significant improvements in the χ^2, the weighted residuals, and the autocorrelation function are observed when the data are fit to a sum of three exponentials. The χ^2 value decreases to 1.4–1.7. The recovered lifetime values at the two emission wavelengths are 19.9, 4.4–4.8, and 0.5–0.6 ns. The pre-exponential

factors and fractional intensities indicate that there is significantly less of the long lifetime component than in the other proteins. As much as 20% of the fractional intensity is from the median, 4-ns, component. It is interesting that the long lifetime component is very similar to the long lifetime component of W57L, and distinctly longer than that of the wild-type protein or the W158F mutant. The median lifetime component is longer than the shortest lifetime component of any of the other proteins, and there is an additional, short-lived component. It is clear that replacement of Lys-58 with Cys results in a significant degree of dynamic quenching of ε-adenylyl GS.

The steady-state emission spectra of the ε-adenylyl group attached to the wild type, the W57L mutant, and the W158F mutant have been combined with the fluorescence parameters of the individual components obtained at the five emission wavelengths to calculate the normalized DAS. These spectra are shown in Figure 5. As expected from the TRES, the individual components are not sufficiently resolved along the wavelength axis to result in a significant time dependence of the spectra. Other than the difference in intensity of the short lifetime component, the DAS are nearly identical for the three proteins.

Quantum yield of ε-AMP bound to GS and mutants

The increase in excited state lifetimes and pre-exponential values of the long lifetime component observed in the W57L mutant suggests that a small degree of dynamic quenching is present, either directly from Trp-57 or from some other part of the Trp-57 loop, where mutation of Trp to Leu reduces this dynamic quenching. The fact that mutation far from the adenylylation site does not result in any quenching suggests that some specific interaction occurs between the Trp-57 loop and the regulatory adenylyl group. The increase in lifetime values in the W57L mutant can be used to predict the relative quantum yields expected for the wild-type protein and W57L GS, in the absence of any other quenching mechanism. The model for physical interaction between ε-AMP and Trp-57 may be described by an equilibrium between open complexes (in which the purine and indole are not in direct contact) and closed complexes (with the purine and indole rings stacked in direct contact with one another). The stacked complexes have vanishingly small quantum yields, and are completely statically quenched. The open complexes fluoresce, but may be dynamically quenched by collision with the indole, or by dipolar relaxations near Trp-57, during the excited state of the ε-purine. That is, measurement of fluorescence lifetimes only provides information about the open complexes, because closed complexes are spectroscopically silent.

If the relative quantum yield of the wild-type protein compared to the W57L mutant was decreased more than expected from the decrease in lifetime values, then this would suggest that a static quenching mechanism was also operative. The fraction of absorption transitions, γ, resulting from the open, unquenched ε-AMP in the ground state, relative to the total number of absorptions is $\gamma = (F/F_0)(\tau_0/\tau)$, where F_0 and τ_0 and F and τ are the quantum efficiency and the excited state lifetimes in the ab-

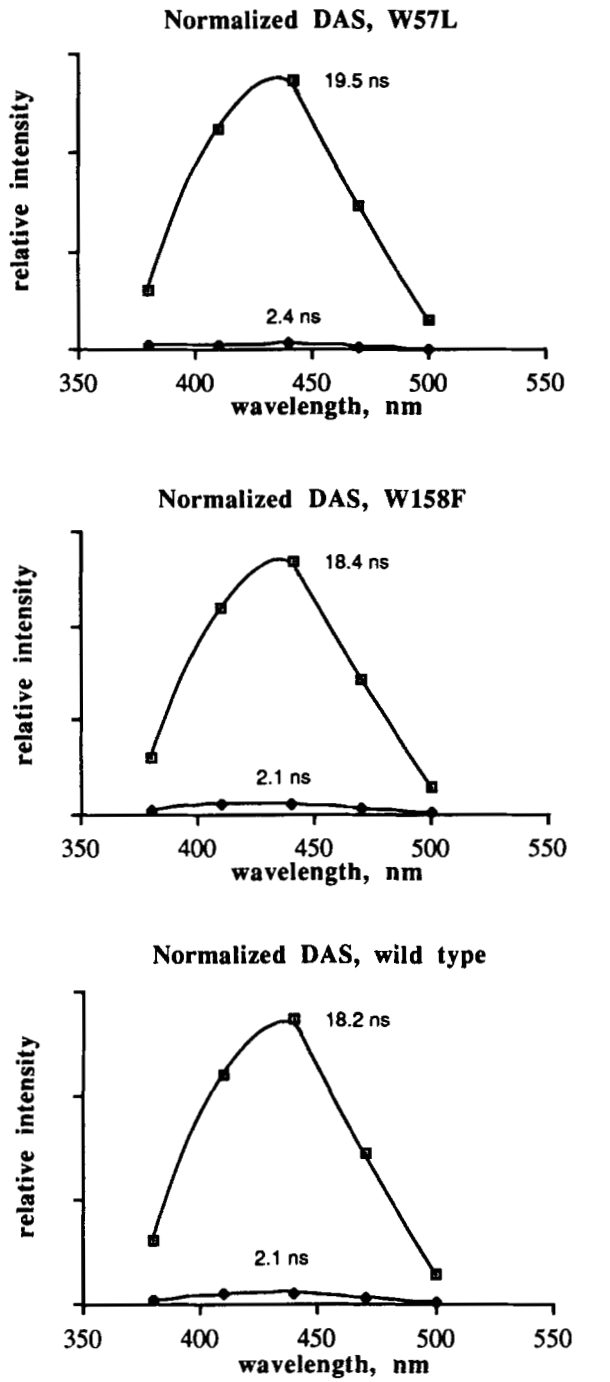

Fig. 5. Decay-associated spectra of ε-adenylylated GS and mutants. The individual lifetime components were constrained to remain the same at each wavelength, and the fractional intensities were combined with the steady-state spectra of each protein.

sence and presence of static quenching. A static quenching of ε-adenylyl would suggest that a (purine)-(tryptophan) dark complex was formed. Due to the low extinction coefficients of the adenylylated proteins at the excitation wavelength, 310 nm, absolute quantum yields were impossible to measure accurately. Also, using shorter excitation wavelengths resulted in tryptophan fluorescence overlapping the emission spectrum of the ε-AMP moiety. Therefore, relative quantum yields were determined by measuring the area under the emission spectra when excited at 310 nm, and dividing this value by the concentration of ε-adenylyl groups in samples of the adenylylated wild-type protein and the adenylylated W57L mutant. Obviously, this does not provide an absolute quantum yield, but assuming that equivalent concentrations of adenylyl groups in identical environments must have the same emission intensity, this affords an accurate relative quantum yield. It was found that the W57L mutant was typically adenylylated with an average of 10.5 ε-AMP groups/dodecamer, whereas the wild-type enzyme was adenylylated an average of 9.5 ε-AMP groups/dodecamer. This was accounted for in samples containing equivalent concentrations of protein by adjusting the integrated emission intensity for this difference. The emission intensity of the W57L mutant was multiplied by 0.91. The proteins were then unfolded in 8 M urea and heated to 40 °C for 3 h, and the emission spectra were integrated again. This ensured that the difference in extent of adenylylation between proteins was accurately accounted for, and that differences in quantum yields were not introduced by different structures in the folded proteins. As shown in Table 2, unfolding the wild-type protein results in a 1.3-fold increase in quantum yield. Unfolding the W57L mutant results in a 1.4-fold increase in quantum yield. Therefore, the difference in adenylylation ratios is not complicated by quenching effects due to differences in the tertiary structure of the two proteins. An important result shown in Table 2 is found in comparison of the relative quantum yields of the folded proteins with the predicted quantum yields based on the difference in excited state lifetime values. The predicted relative quantum yields of the wild-type protein and W57L mutant, Q_{wt}/Q_{57L}, were obtained by assuming direct proportionality between the average lifetimes and the total emission intensity: $Q = k_r \sum \alpha_i \tau_i = k_r \langle \tau \rangle$, where α_i and τ_i are the pre-exponential factors and lifetime values of the ith individual lifetime component of the wild-type and mutant proteins, k_r is the radiative rate constant, and $\langle \tau \rangle$ is the average excited state lifetime. That is, if the radiative rate constants of the ith species are the same, then there is a linear relationship between the quantum yield and the average lifetime (Harris & Hudson, 1990). The proposal that the radiative rate constants are the same for ε-AMP bound to wild-type and mutant GS is supported by the identical steady-state spectra observed for each adenylylated protein. Changes in the excited electronic state would be expected to lead to changes in the emission spectra. More importantly, the DAS of the W57L mutant and the wild-type protein (Fig. 5) are nearly superimposable except for the larger proportion of the short lifetime component in the wild-type enzyme. If a mechanism other than dynamic quenching was present, the spectra of the individual lifetime components would be expected to be different for the wild type versus the W57L mutant. We assume that the major nonradiative mechanism for depopulation of the excited state is through dynamic quenching due to neighboring protein residues. The difference in measured lifetime values and pre-exponential factors (Table 1) would predict a decrease in quantum yield of 12–14% for the wild-type protein relative to the W57L mutant. This is exactly what is observed, suggesting that no additional static quenching mechanisms are operative in the wild-type enzyme.

Table 2. *Relative quantum yields for ε-AMP adenylylated proteins*[a]

Protein	Quantum yield		Predicted yield: from lifetimes
	Native structure	Unfolded	
Wild type	0.85 ± 0.02	1.3	0.87
W57L	1.0	1.4	1.0

[a] All quantum yields were determined as described in Materials and methods, and have been normalized to the quantum yield of the ε-AMP-W57L in the native state. Excitation was at 310 nm. Measurements were performed in 50 mM Hepes, pH 7.5, 100 mM KCl, 25 mM $MgCl_2$.

Tryptophan fluorescence

Any "dark" complex formed from (ε-purine)-(Trp-57) stacking is also expected to result in quenching of the Trp-57 fluorescence (Mutai et al., 1975). Therefore, the relative quantum yields and excited state lifetimes were also considered for the tryptophan emission of the wild-type, W158F, and W57L proteins. Here, the proteins adenylylated with either AMP or the ε-AMP were used. Comparison of the quantum yield for Trp-57, in the presence and absence of an adenylyl group, is complicated by the possibility of conformational changes resulting from adenylylation that alter fluorescent properties of this tryptophan, independent of specific interactions between the purine ring and the indole. Also, the contribution of Trp-158 fluorescence in the wild-type emission makes comparison of wild-type and W158F proteins as a function of adenylylation state meaningless. However, several qualitative observations concerning the tryptophan fluorescence of these proteins are consistent with the proposal that a stacked, "dark" complex between Trp-57 and the bound AMP moiety is not formed. The steady-state emission intensity of Trp-57 does not decrease when the pro-

tein is adenylylated. In fact, the quantum yield of the W158F mutant and wild-type GS is increased slightly (10%) when these enzymes are adenylylated. Although the physical source of this difference is impossible to determine without additional information concerning the conformation of the adenylylated enzyme, it is clear that when the adenylyl group is covalently attached to Tyr-397, Trp-57 retains a nearly identical quantum yield. Also, the excited state lifetimes of Trp-57 (W158F mutant) have been determined for low-adenylylation and high-adenylylation state samples. Detailed analysis of the tryptophan emission of the wild-type protein and the W158F and W57L mutants has been previously reported (Atkins et al., 1991; Atkins & Villafranca, 1992). Comparison of the excited state lifetime values of Trp-57 for W158F of adenylylation states $n = 4$ and $n = 11$ indicates no significant decrease in the recovered lifetime values and, in fact, a slight increase. These results are summarized in Table 3. Similar results were obtained with the wild-type protein.

An additional approach to search for (Trp-57)–(adenylyl) interactions included the examination of excitation spectra of adenylylated GS and mutants. Although nucleotides have very short excited state lifetimes and therefore fluoresce very weakly, their contact with indoles has been detected by energy transfer to the indole by the contribution of a band at 254–256 nm in the excitation spectra of the indole (Weber, 1960). Excitation spectra of low-adenylylation state samples were compared to those of high-adenylylation state samples for the wild type, the W57L mutant, and the W158F mutant. Adenylylation did not result in a detectable contribution to the excitation spectra in the 260-nm region of any of these proteins (data not shown).

In addition to protein samples with covalently bound AMP, studies of the steady-state tryptophan fluorescence of the wild-type protein and the W158F mutant adenylylated with ε-AMP were performed. As with the AMP moiety, the ε-AMP group did not significantly reduce the fluorescence intensity of Trp-57.

Table 3. *Fluorescence lifetimes of Trp-57 as a function of adenylylation state*[a]

Adenylylation state	τ (ns), α at wavelength		
	320 nm	340 nm	360 nm
$n = 4$	5.38, 0.25	5.65, 0.21	5.56, 0.29
	1.63, 0.47	1.83, 0.34	1.95, 0.43
	0.29, 0.28	0.35, 0.45	0.29, 0.28
	$\chi^2 = 1.98$	$\chi^2 = 1.73$	$\chi^2 = 2.01$
$n = 11$	5.43, 0.22	5.76, 0.21	5.41, 0.30
	1.79, 0.40	1.76, 0.41	1.83, 0.40
	0.35, 0.38	0.36, 0.35	0.28, 0.29
	$\chi^2 = 1.61$	$\chi^2 = 1.55$	$\chi^2 = 1.54$

[a] n equals the average number of adenylyl groups bound per dodecamer. Excitation was at 295 nm. Conditions were as in Table 1.

Enzyme activity

In order to determine whether the effects of Trp-57 and surrounding structure on the fluorescence of ε-AMP are correlated to any functional aspects, the regulatory efficacy of the adenylyl group bound to the W57L and K58C mutants was compared to the wild-type protein. A frequently used measure of GS activity is the γ-glutamyl transferase assay, which involves GS-catalyzed formation of γ-glutamylhydroxamate. Adenylylation of wild-type GS results in a selective decrease in the γ-glutamyl transferase assay that contains Mg^{2+} in addition to the Mn^{2+} found in the standard assay. A second assay that is used to determine GS activity is a coupled assay in which consumption of ATP occurs simultaneously with oxidation of NADH. As with the transferase assay, the Mg-containing wild-type adenylylated enzyme is nearly completely inhibited in this biosynthetic assay (Ginsburg et al., 1970). Both W57L and K58C mutants demonstrate "normal" activity upon adenylylation in each of these assays. These results are summarized in Table 4. It is clear that the dynamic fluorescence quenching of the ε-AMP group that is attributable to the Trp-57 loop does not directly play a role in the regulatory function. Examination of the K_m values for ATP and the k_{cat} for glutamine synthesis indicates, however, that the Trp-57 loop plays a role in binding this substrate and a role in catalysis. In particular, it appears that Lys-58 has a significant role in stabilization of enzyme-bound intermediates, because mutation of this residue causes a 20-fold reduction in k_{cat} and only a 3-fold increase in the K_m for ATP.

Computational studies

These studies were conducted in order to provide a model to assist in explaining the fluorescence and enzyme activ-

Table 4. *Regulation of enzyme activity by adenylylation*

Protein[a]	Transferase activity, Mn^{2+} (units/mg)	Biosynthetic assay, Mg^{2+} (units/mg)	K_m (ATP) (μM)
WT, $n = 1.5$	119 ± 8	39	139 ± 9
WT, $n = 12.3$	122 ± 12	0.8	ND[b]
W57L, $n = 1.9$	99 ± 7	24	332 ± 21
W57L, $n = 10.9$	93 ± 9	0.8	ND
K58C, $n = 0.9$	14 ± 4	2.1	451 ± 61
K58C, $n = 11.4$	15 ± 8	0.08	ND

[a] The average adenylylation state (n) was determined by measuring release of P_i following acid hydrolysis of protein samples and by the γ-glutamyl transferase assay (Woolfolk et al., 1966). The average of these values is reported in the table. WT, wild type.

[b] ND, not determined due to low enzymatic activity.

ity results presented above. To determine if stacking of Trp-57 and adenine of the covalent Tyr-397-adenyl group was a favorable interaction, calculations of total potential energies for adenylylated GS were obtained at points along a pathway from extended to parallel, stacked conformations of Trp-57 and adenine. The resulting trend shows fluctuations (between 0.5 and 2% of the total energy) in a nondirectional order from 9 to 3 Å (distance between rings), with the nonbonded electrostatic term being the dominant factor. Starting calculations beginning with stacked structures (with the rings 3 and 4 Å apart) and allowing conformational relaxation resulted in a nonparallel, translated conformation for the two rings that settled at an average separation of about 5 Å (Fig. 6A). In addition, the relative energy changes were in a more favorable direction, with the nonbonded terms (electrostatic and van der Waals) responsible for the shift.

Molecular dynamics simulations of the parallel, stacked conformation of GS as the initial structure depicted the two rings drifting apart to assume a near-perpendicular orientation (average ring separation approx. 5.5 Å), independent of the heating rate (0.1 or 0.5 K per step) or length of simulation (1.5 or 5.0 ps) (Kinemage 2). The Trp-57 indole ring appeared to settle in a groove formed by the entire adenylylated moiety (tyrosine, phosphoryl group, and adenosine), in which the indole amino hydrogen is interacting with the ribose ring oxygen (hydrogen-bond distance <3 Å). Dynamics animation of the 8-Å extended form of GS, however, showed the two rings drifting apart even further; the hydrogen-bonded conformation was never sampled.

The K58C mutant GS was subjected to dynamic simulation in order to test for potential conformations that could help explain this enzyme's shorter excited state lifetimes for ε-AMP. The cysteine sampled an environment in which the Cys sulfur to AMP ring distance was shorter than the Lys-Cγ to AMP ring closest approach (10.9 vs. 13.3 Å); however, there was no evidence for the cysteine ever making direct contact with the adenylyl group. However, there appeared to be a shift in the position of the adenylyl group (2.5 Å average displacement) relative to the wild-type enzyme. In addition, the potential hydrogen bond (Trp-57 to ribose discussed above) observed for the wild-type enzyme was not evident in the K58C mutant (average N → O distance >7 Å). It must be noted that these computational results are based on the currently available crystal structure for GS in which Lys-58 is represented as pointing in toward the active site of the neighboring subunit; precise lysine positions are notorious for being difficult to characterize due to their high mobility.

Distance targeting (6–2 Å) of a model compound representing the adenine and indole rings (3-(indol-1-yl)propyladenine, ind-C_3-ade; Fig. 7) yielded a potential energy trend, with the optimum parallel, stacked conformation lying between 3 and 4 Å (Fig. 6B). When each of these stacked species was allowed to relax, both converged to approximately the same energy and position at 3.5 Å (ring to ring). In addition, the 5-Å stacked conformation settled at the 3.5-Å position after simulation. A similar "equilibrium" conformation was attained upon immersing the 3-Å stacked species in water and allowing the solvated species to relax.

Similar data were acquired from molecular dynamics simulations of parallel and stacked or near-stacked conformations of ind-C_3-ade. The indole and adenine rings in the 3.5-Å structure did not drift apart during heating, equilibration, and simulation; however, under similar conditions (0.5 K/step heating rate), the 5-Å near-stacked structure approached and held the 3.5-Å conformation. Under conditions of 1 K/step heating rate and a total dynamics run time of 2.9 ps, the fully extended form of the model settled in the <4-Å parallel, stacked conformation.

Discussion

Glutamine synthetase is regulated in some prokaryotes by adenylylation of a specific tyrosine residue (Tyr-397 in *E. coli*). In the present study, wild-type GS and site-directed mutants have been specifically adenylylated at Tyr-397 with the fluorescent probe ε-AMP. These studies were performed in order to define possible interactions between the covalently bound adenylyl group and the Trp-57 loop in the adjacent subunit. The measurement of fluorescent lifetimes and quantum yields provided dynamic and struc-

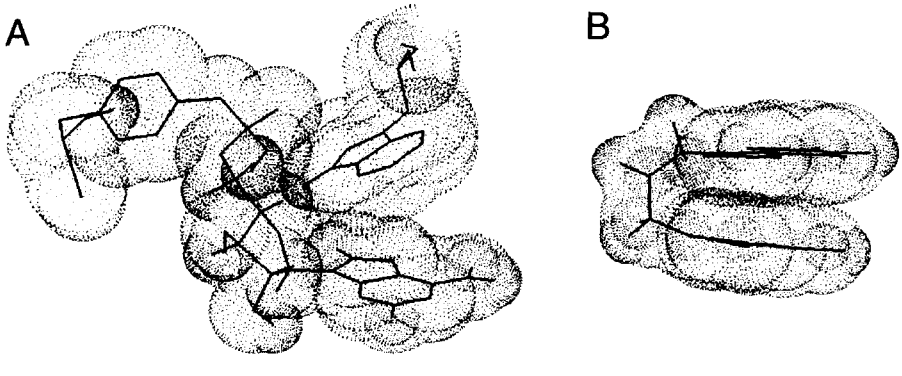

Fig. 6. Van der Waals representation of the end products of the dynamic simulations for adenylylated wild-type GS (**A**) and ind-C_3-ade (**B**). Initial structures contained the indole and purine rings in parallel, stacked conformations; fully extended ind-C_3-ade also achieved this final conformation.

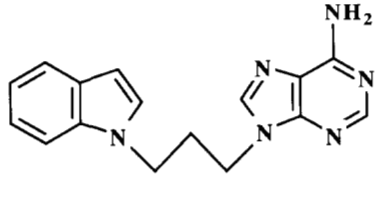

Fig. 7. Structure of 3-(indol-1-yl)propyladenine (ind-C_3-ade).

tural information concerning these interactions; the results presented herein provided a model for the mechanism of regulation of GS activity by adenylylation.

The finding that ε-AMP attached to Tyr-397 exhibits heterogeneous fluorescence decay kinetics is most likely the result of ground-state heterogeneity arising from microconformational states sampled by the probe. Many single-tryptophan-containing proteins exhibit heterogeneous fluorescence decay kinetics (Hutnik & Szabo, 1989a,b; Royer et al., 1990; Atkins et al., 1991), and the results presented here with a single, long-lifetime probe attached at a specified location on each GS subunit demonstrate the utility of non-amino acid labels as probes of protein dynamics. Both of the lifetime values recovered for the adenylyl group attached to the wild-type protein are shorter than the single lifetime value found for the free probe, indicating that the bound adenylyl group is not completely solvent-exposed, and some interaction with protein residues is apparent. Although the fractional intensities indicate that the majority of the fluorescent species retain a long lifetime, 18 ns, this is significantly shorter than the 22 ns recovered for the free probe. The second recovered lifetime value, 2 ns, is much shorter, indicating that the majority of bound AMP groups are not directly adjacent to protein residues that dynamically collide with them. Most adenylyl groups only occasionally collide with protein residues or come close enough to be quenched by dipolar relaxations. A fraction of the adenylyl groups, however, are very efficiently quenched and interact with protein residues nearly immediately after reaching the excited state. These results are consistent with previously published results from NMR and fluorescence studies (Villafranca et al., 1978). The previous results also indicated that the purine ring of the bound adenylyl groups was relatively mobile, with faster rotational correlation times than the entire dodecamer. Thus, the adenine ring probably does not collide with amino acid residues frequently enough to restrict its motion.

At least part of the dynamic quenching that is observed for bound ε-AMP groups, and presumably the collisional interaction with protein residues, is directly attributable to the Trp-57 loop. Mutation at either Trp-57 or Lys-58 affects the fluorescence decay kinetics, whereas mutation at a distant site, Trp-158, has no effect. The Trp-57 mutant is characterized by slightly longer fluorescent lifetimes and a higher proportion of the longer lifetime component than the wild-type protein. This indicates that Trp-57 and the purine ring of bound adenylyl groups directly interact through collisional quenching, or Trp-57 is responsible for some structural character that allows the adenylyl groups to be quenched by other residues when the indole is removed. When the sterically bulky Trp-57 is replaced by Leu, the ε-AMP fluorescence decay kinetics resemble the free ε-AMP.

The results obtained with the K58C mutant are noteworthy because the effect on the ε-AMP decay kinetics is opposite to the effect observed with the W57L mutant. The K58C mutant has a significantly shorter-lived average excited state than both wild type and the W57L mutant adenylylated with ε-AMP. Several explanations are plausible. It is noteworthy that cysteine has been reported to act as an efficient dynamic quencher of several types of fluorophores (Steiner & Kirby, 1969; Harris & Hudson, 1990), and mutation of Lys-58 to Cys may simply provide a thiol quencher near the adenylyl group. This does not seem likely because the side chain of Lys-58 appears to point toward the active site, away from the site of adenylylation. In order for Cys-58 to directly collide with the adenylyl group, some structural change would have to take place to allow the side chain of Cys-58 to point away from the active site, or to allow the adenylyl group to be pulled inward toward it. Alternatively, the drastic mutation in which a positively charged Lys residue is replaced with a neutral, much shorter Cys side chain may cause structural perturbation of the Trp-57 loop such that the ε-AMP group lies in a completely different environment than in the wild-type or W57L proteins, where this environment allows for more efficient dynamic quenching by other protein residues. Whereas a positively charged Lys-58 may form a specific ion pair or hydrogen bond with phosphoryl oxygens or hydroxyl groups on the sugar moiety of the adenylyl group, a Cys residue at position 58 may allow the purine ring of ε-adenylyl groups to adopt conformations that result in efficient quenching. Whether the effect of Cys-58 is due to direct collisional quenching or indirect effects resulting from microconformational changes, the results indicate that the Trp-57 loop lies in close proximity to the ε-AMP bound at Tyr-397.

Although the Trp-57 loop provides a dynamic quenching mechanism for the adenylyl group, and apparently lies within a distance that allows for direct collisional interaction, there is no evidence from the current study to indicate that a (purine)-(indole) complex between the adenine ring and Trp-57 is formed. If a significant fraction of the ε-AMP groups were stacked with the Trp-57, then the decrease in the relative quantum yield of the adenylyl group bound to wild-type GS compared to the W57L mutant would be expected to be more than the decrease observed due to dynamic quenching. This is because a (purine)-(indole) complex is statically quenched

and does not fluoresce. The difference in relative quantum yields determined for the ε-AMP group bound to wild-type GS and the W57L mutant is completely accounted for by the dynamic quenching provided by Trp-57; no evidence for static quenching or additional mechanisms of quantum yield decrease is apparent. It is possible that adenylyl groups on adjacent hexameric rings are stacked with one another rather than with Trp-57, and that mutation at Trp-57 or Lys-58 does not affect this interaction. This seems unlikely, since (purine)–(purine) stacking also results in a nonfluorescent complex, and adenylylated proteins clearly fluoresce with quantum yields that are similar to the quantum yield of free adenylyl groups. An additional approach that may detect (purine)–(purine) stacking is circular dichroism, since stacked ε-nucleosides demonstrate an intense negative CD band in the far UV (Tolman et al., 1974).

In addition to the fluorescence decay kinetics of the ε-AMP groups, the fluorescence properties of Trp-57 in high- and low-adenylylation states have been compared. The fluorescence decay kinetics of *E. coli* Mn^{2+}-GS have been extensively documented elsewhere (Atkins et al., 1991; Atkins & Villafranca, 1992). The Mg-enzyme has nearly identical decay characteristics, and comparison of the fluorescence parameters of Trp-57 for high- and low-adenylylation states indicates no dynamic quenching due to the adenylyl group. Furthermore, the quantum yield of Trp-57 in the adenylylated enzyme is at least as large as in the unadenylylated enzyme, consistent with the proposal that Trp-57 and adenine rings are not stacked in a specific complex.

The enzyme activity of the mutant proteins compared to the wild-type GS suggests that the dynamic quenching that is attributable to the Trp-57 loop is not directly associated with the physiological function of the adenylyl group. In both the γ-glutamyl transferase assay and the Mg-biosynthetic assay, the W57L and K58C mutants demonstrate nearly complete down-regulation of enzyme activity when adenylylated. The role of the Trp-57 loop in binding ATP has been documented (Atkins et al., 1991; Atkins & Villafranca, 1992). The results included here extend the previous studies and demonstrate that Lys-58 plays a direct role in binding ATP and intermediates formed during catalysis. In the Mg-biosynthetic assay, ADP release is the rate-limiting step of GS catalysis. More detailed kinetic experiments are required to determine if the large decrease in k_{cat} for the K58C mutant is due to a decrease in the rate of ADP release or whether other catalytic steps become rate-limiting.

The amino acid sequence surrounding Trp-57 (Gly-Ser-Ser-Ile-Gly-Gly-Trp^{57}-Lys-Gly) is very similar to consensus sequences of glycine-rich, nucleotide-binding domains found in several proteins. These flexible loops contain the sequence Gly-X-Gly-X-X-Gly-Lys or Gly-X-X-X-X-Gly-Lys. It has been shown that in such loops, the invariant Lys residues are directly involved in binding phosphoryl oxygens (Redfield & Papastavros, 1990). Notably, the magnitude of the change in fluorescence parameters of Trp-57 that occurs when ATP binds to the unadenylylated Mg-enzyme is greatly diminished when the enzyme is adenylylated. Apparently, the adenylyl groups interfere with ATP binding, or they inhibit the conformational changes that normally accompany ATP binding. We have considered the possibility that the adenylyl group provides a covalently bound moiety that could serve as a competitive inhibitor in the substrate ATP pocket. The adenylyl group acting in this manner could interact with the Trp-57 loop, preventing the substrate from binding. The kinetic data with the K58C mutant further support the role of the Trp-57 loop in ATP binding, and the binding of transition-state complexes or chemical intermediates formed during catalysis. However, the results presented here also indicate that Trp-57 and Lys-58 are not essential for the regulatory behavior of covalently bound adenylyl groups (changes in kinetic parameters). Therefore, it is not likely that the adenylyl groups directly compete for ATP binding sites, or they compete for a part of the ATP binding site other than the Trp-57 loop.

Computational studies were performed with the intent of lending support to the fluorescence and enzyme activity data, as well as to offer insight into the mode of communication of the adenylyl group with the active site of adenylylated GS. These studies suggested that a parallel, stacked conformation is never freely sampled during the course of a dynamics simulation in cases starting with an extended form of the enzyme (i.e., Trp-57 indole and modified Tyr-397 adenine rings >6 Å apart). Forcing the molecule into this conformation by applying distance targets provided no obvious increase in stability; indeed, allowing the stacked structure to relax, either by minimization or a dynamics sequence, invariably resulted in a displaced, near-perpendicular conformation (Kinemage 2). These results corroborate the above-mentioned findings of an absence of a parallel, stacked ring species. In addition, the computational studies offered a potential indole–ribose interaction in the form of a hydrogen bond between the nitrogen and ribose ring oxygen (<3 Å). No evidence was found for the adenylyl group competing for or interacting with any other component of the ATP binding site. Unlike GS, the ind-C_3-ade model appeared to be "comfortable" in a stacked conformation, based on the minimization and molecular dynamics studies, in agreement with previously reported fluorescence data (Mutai et al., 1975). A minimum potential energy was calculated to lie at a point between 3 and 4 Å, corresponding to parallel stacking. Under conditions of relatively rapid heating, this stacked species was generated from the fully extended (planar) form of the molecule, providing further evidence for the validity of this conformation. The results of the K58C experiment point toward structural perturbation being the more reasonable hypothesis for explaining the

shorter-lived excited state lifetimes of this enzyme. No evidence for direct Cys-58/AMP-ring contact was presented.

Taken together, these results suggest that adenylyl groups attached to Tyr-397 directly interact with the Trp-57 loop, but do not form a (purine)–(indole) ring stacked complex. This raises several possibilities concerning the mechanism of regulation of GS activity by adenylylation. It is possible that the purine ring of attached AMP residues is required for regulation of enzyme activity and that the adenine ring specifically interacts with a region of the protein other than the Trp-57 loop. However, the previously reported results that indicate that the adenine ring is highly mobile, along with the dynamic quenching and computer analyses included here, suggest that the adenine ring does not strongly interact with protein residues to the extent that it is rigidly held in close contact with specific amino acids. It is possible that the phosphoryl group and/or the sugar moiety of the attached AMP groups maintain specific interactions with protein residues that are sufficient to prevent the enzyme from undergoing specific conformational changes associated with catalysis. If this is the case, then the adenine ring of the adenylyl groups may be nonessential for regulation of GS activity. It is interesting that preliminary results with phosphorylated GS, in which the adenosyl group has been enzymatically removed from the adenylylated enzyme, indicate that the phosphotyrosyl group is sufficient to provide regulation of GS catalysis (Kimura et al., 1986). Rigorous identification of phosphotyrosine-397 and the catalytic properties of GS containing this species remain to be established, however. Finally, it is possible that the AMP groups simply sterically block a substrate access channel without close contact with other protein residues.

Materials and methods

Site-directed mutagenesis

The W57L and W158F mutant proteins were constructed, expressed, and purified as previously described (Atkins et al., 1991). The K58C mutant was constructed by the method of Taylor et al. (1985) with an in vitro site-directed mutagenesis kit purchased from Amersham. The kit was used without modification, except that the single-stranded template used for mutagenesis was obtained from the phagemid pBL88.

Adenylylation of proteins

ε-ATP was purchased from Molecular Probes (Eugene, Oregon). Wild-type and mutant GS were adenylylated with ε-AMP using partially purified ATase, kindly provided by Dr. S.G. Rhee, NIH. Typically, a 2–3-mL sample of 30–40 μM (subunits) GS was dialyzed against 50 mM Tris, pH 8.0, 25 mM $MgCl_2$. The samples were made 30 mM in glutamine, 5 mM ε-ATP, and 2–3 μL of ATase stock solution (approx. 1 mg/mL) was added. The samples were incubated at 37 °C, and the progress of adenylylation was monitored with the γ-glutamyl transferase assay (Woolfolk et al., 1966). Typically, reaction was complete within 3–4 h. The reaction was incubated at 48 °C for an additional 25 min in order to inactivate the ATase and avoid subsequent deadenylylation. The samples were neutralized and brought to 50 mM $MgCl_2$ by addition of 200–300 μL of 1.0 M Tris, pH 7.0, 2.5 mM $MgCl_2$. Samples were made 2 mM in Zn^{2+} by dropwise addition of 0.1 M $ZnCl_2$. The precipitated GS was separated by centrifugation, and the pellet was washed with 50 mM Tris, pH 7.0, 50 mM $MgCl_2$, 2 mM $ZnCl_2$ to remove free ε-ATP and centrifuged again. The pellet was resuspended in 1–2 mL of the same buffer and dialyzed against 1 L 50 mM Hepes, pH 7.2, 10 mM EDTA, 100 mM KCl, 50 mM $MgCl_2$ to remove Zn^{2+}. Samples were then dialyzed against 4 L of 50 mM Hepes, pH 7.2, 100 mM KCl, 25 mM $MgCl_2$ and used within 24 h in fluorescence experiments. These centrifugation and exhaustive dialysis steps were sufficient to remove any remaining free ε-ATP. The adenylylation state of all samples was confirmed by the transferase assay after fluorescence experiments to ensure that no ε-AMP had hydrolyzed during sample preparation or storage. Protein concentrations were determined by the BCA assay (Pierce Chemicals) after removal of Mn^{2+} and by the method of Edelhoch (1967), which relies on known extinction coefficients of tryptophan, tyrosine, and cysteine in 6 M guanidinium hydrochloride.

Fluorescence measurements

Fluorescence lifetimes were measured with a Photon Technology International (PTI) LS100 time-correlated single photon-counting fluorimeter, using 256 total channels for data collection. The system was calibrated to be 1,339 ps/channel. Excitation was at 310 or 295 nm with a flash lamp purged with 30% nitrogen in helium at 15 psi. For each emission wavelength, 15,000 counts were obtained in the peak channel, with lamp profile calibrated every 2,000 counts. Slit widths were 5 mm. Lamp profile was obtained from light scattered with a standard glycogen solution. Steady-state fluorescence measurements were made on the same instrument using the steady-state mode. For quantum yield determinations, slit widths were kept at 3 mm or less, and total optical density at the wavelength of excitation was kept below 0.06 OD. Before integration, the emission spectra were corrected for the wavelength dependence of the emission monochromater.

Computational studies

All minimizations and molecular dynamics trajectories were calculated on a Silicon Graphics Iris 4D/240GTX

computer utilizing QUANTA/CHARMM software supplied by Polygen/MSI. "Covalent attachment" of the AMP moiety to Tyr-397 (Tyr-O-P-AMP) in one of the 12 subunits was accomplished using the appropriate subroutines in QUANTA. The size of dodecameric GS (>600 kDa) precluded use in its entirety for calculations; therefore, a portion limited by a 25-Å radius centered around the AMP-phosphorus added to a 15-Å radius centered around the unadenylylated Tyr-397-oxygen in a diagonally located subunit was examined. Hydrogens were added to this starting structure and allowed to relax using the steepest descents algorithm, followed by a "spin" of the AMP to obtain the optimum steric conformation. Relaxation of the entire adenylylated model resulted in minimal alteration of atom positions. All minimizations (unless otherwise noted) were performed using the adopted basis set Newton–Raphson algorithm with a 1×10^5 iteration limit (never reached), and energy gradient tolerance and energy value tolerance of 0.01 and 0.00, respectively. Atoms located outside a sphere of 22 Å around the AMP-phosphorus were totally constrained; this included the ends of both the Tyr-397 and the Trp-57 loops.

The first set of minimization studies focused on determining changes in potential energy as the purine and Trp-57 rings approached one another. This was accomplished by targeting corresponding pairs of atoms in each ring system to successively shorter distances (6–3 Å, at 1-Å intervals), i.e., approaching a parallel stacking position. The second set of minimization studies allowed each of the aforementioned "stacked" structures to relax, in order to educe the most favorable conformation. No solvent was included in any of these studies. Identical conditions were employed, where applicable, for analysis of the indole-$(CH_2)_3$-adenine model, and calculations were performed with and without immersion in water.

Molecular dynamics studies of the GS model began with heating the 3-Å stacked structure (or the extended structure) from 0 to 300 K in 3,000 steps at a rate of 0.001 ps/step (0.1 K/step). Equilibration occurred over 1,000 steps followed by 5,000 steps of simulation, all at 0.001 ps/step, yielding a total sampling time of 9 ps. In a separate experiment, heating was conducted at a rate of 0.5 K/step, with a total sampling time of 4.7 ps. The K58C mutation was performed on the 3-Å stacked structure and dynamics animation was created as described for 9 ps. Molecular dynamics trajectories of the indole-$(CH_2)_3$-adenine model were calculated using both the extended and stacked forms as starting points, with heating rates of 0.5 and 1 K/step and total times of 1.8 and 2.9 ps, respectively.

Acknowledgments

W.M.A. is supported by NIH grant GM-13714, and J.J.V. is supported by NIH grant GM-23529.

References

Abell, L.M. & Villafranca, L.M. (1991). Effect of metal ions and adenylylation state on the internal thermodynamics of phosphoryl transfer in the *Escherichia coli* glutamine synthetase reaction. *Biochemistry 30*, 1413–1418.

Alcala, J.R., Gratton, E., & Prendergast, F.G. (1987). Interpretation of fluorescence decays in proteins using continuous lifetime distributions. *Biophys. J. 51*, 925–936.

Almassy, R.J., Janson, L.A., Hamlin, R., Xuong, N.-H., & Eisenberg, D. (1986). Novel subunit-subunit interactions in *Escherichia coli* glutamine synthetase. *Nature 323*, 304–309.

Atkins, W.M., Stayton, P.S., & Villafranca, J.J. (1991). Time resolved fluorescence studies of genetically engineered *E. coli* glutamine synthetase. Effects of ATP on the Trp-57 loop. *Biochemistry 30*, 3406–3416.

Atkins, W.M. & Villafranca, J.J. (1992). Time resolved fluorescence studies of tryptophan mutants of *E. coli* glutamine synthetase: Conformational analysis of intermediates and transition state complexes. *Protein Sci. 1*, 342–355.

Beechem, J.M., Knutson, J.R., Ross, A., Truner, B.W., & Brand, L. (1983). Global resolution of heterogeneous decay by phase/modulation fluorometry: Mixtures and proteins. *Biochemistry 22*, 6054–6058.

Chock, P.B., Huang, C.Y., Timmons, R.B., & Stadtman, E.R. (1973). ε-Adenylylated glutamine synthetase: An internal fluorescent probe for enzyme conformation. *Proc. Natl. Acad. Sci. USA 70*, 3134–3138.

Edelhoch, H. (1967). Spectroscopic determination of tryptophan and tyrosine in proteins. *Biochemistry 5*, 1948–1954.

Ginsburg, A., Yeh, J., Hennig, S.B., & Denton, M.D. (1970). Some effects on the biosynthetic properties of the glutamine synthetase from *Escherichia coli*. *Biochemistry 9*, 633–648.

Gruber, B.A. & Leonard, N.J. (1975). Dynamic and static quenching of 1,N^6-ethenoadenine fluorescence in nicotinamide 1,N^6-ethenoadenine dinucleotide and in 1,N^6-etheno-9-[3-(indole-3-yl)propyl]adenine. *Proc. Natl. Acad. Sci. USA 72*, 3966–3969.

Harris, D.L. & Hudson, B.S. (1990). Photophysics of tryptophan in bacteriophage T4 lysozymes. *Biochemistry 29*, 5276–5285.

Hutnik, C.M. & Szabo, A.G. (1989a). Confirmation that multiexponential fluorescence decay behavior of holoazurin originates from conformational heterogeneity. *Biochemistry 28*, 3923–3934.

Hutnik, C.M. & Szabo, A.G. (1989b). A time-resolved fluorescence study of azurin and metalloazurin derivatives. *Biochemistry 28*, 3935–3939.

Jameson, D.M., Gratton, E., & Hall, R.D. (1984). The measurement and analysis of heterogeneous emissions by multifrequency phase and modulation. *Fluorometry Appl. Spectrosc. Rev. 20*, 55–106.

Kimura, K., Kaizu, Y., Matsuoka, K., & Nakano, Y. (1986). The conversion of adenylylated glutamine synthetase into phosphotyrosine enzyme by micrococcal nuclease. *Biochem. Biophys. Res. Commun. 137*, 716–721.

Liou, R.-S. & Anderson, S.R. (1978). Binding of ATP and of 1,N^6-ethenoadenosine triphosphate to rabbit muscle phosphofructokinase. *Biochemistry 17*, 999–1004.

Mutai, K., Gruber, B.A., & Leonard, N.J. (1975). Synthetic spectroscopic models. Intramolecular stacking interactions between indole and connected nucleic acid bases. Hypochromism and fluorescence. *J. Am. Chem. Soc. 97*, 4095–4104.

Pesole, G., Bozzetti, M.P., Lanave, C., & Saccone, C. (1991). Glutamine synthetase gene evolution: A good molecular clock. *Proc. Natl. Acad. Sci. USA 88*, 522–526.

Redfield, A.G. & Papastavros, M.Z. (1990). NMR study of phosphoryl binding loop in purine nucleotide proteins: Evidence for a strong hydrogen bond in human N-ras protein. *Biochemistry 29*, 3509–3514.

Rhee, S.G., Ubom, G.A., Hunt, J.B., & Chock, P.B. (1982). Catalytic cycle of the biosynthetic reaction catalyzed by adenylylated glutamine synthetase from *Escherichia coli*. *J. Biol. Chem. 257*, 289–297.

Royer, C.M., Gardner, J., Beechem, J.M., Brochon, J.C., & Mathews, K.S. (1990). Resolution of the intrinsic fluorescence decay kinetics of the two tryptophan residues of *E. coli* Lac repressor using genetically engineered single tryptophan mutants. *Biophys. J. 58*, 363–378.

Secrist, J.A., Barrio, J.R., Leonard, N.J., & Weber, G. (1972). Fluorescent modification of adenosine-containing coenzymes. Biologi-

cal activities and spectroscopic properties. *Biochemistry 11*, 3499–3506.

Shapiro, B.M., Kingdon, H.S., & Stadtman, E.R. (1967). Regulation of glutamine synthetase, VII. Adenylyl glutamine synthetase: A new form of the enzyme with altered regulatory and kinetic properties. *Proc. Natl. Acad. Sci. USA 58*, 642–649.

Spencer, R.D., Weber, G., Tolman, G.L., Barrio, J.R., & Leonard, N.J. (1974). Species responsible for the fluorescence of 1:N^6-ethenoadenosine. *Eur. J. Biochem. 45*, 425–429.

Steiner, R.F. & Kirby, E.P. (1969). The interaction of the ground and excited states of indole derivatives with electron scavengers. *J. Phys. Chem. 73*, 4130–4135.

Taylor, J.W., Ott, J., & Eckstein, F. (1985). The rapid generation of oligonucleotide-directed mutations at high frequency using phosphothiorate DNA. *Nucleic Acids Res. 13*, 8764–8785.

Tolman, G.L., Barrio, J.R., & Leonard, N.J. (1974). Chloroacetaldehyde-modified dinucleoside phosphates. Dynamic quenching and quenching due to intramolecular complexation. *Biochemistry 24*, 4869–4878.

Villafranca, J.J., Rhee, S.G., & Chock, P.B. (1978). Topographical analysis of regulatory and metal ion binding sites on glutamine synthetase from *Escherichia coli*: ^{13}C and ^{31}P nuclear magnetic resonance and fluorescence energy transfer study. *Proc. Natl. Acad. Sci. USA 75*, 1255–1259.

Weber, G. (1960). Fluorescence polarization spectrum and electronic energy transfer in tyrosine, tryptophan, and related compounds. *Biochem. J. 75*, 335–345.

Wierenga, R.K., Terpstra, P., & Hol, W.G.J. (1986). Prediction of the occurrence of the ADP-binding bab-fold in proteins using an amino acid sequence. *J. Mol. Biol. 187*, 101–107.

Woolfolk, C.A., Shapiro, B.M., & Stadtman, E.R. (1966). Regulation of glutamine synthetase 1. Purification and properties of glutamine synthetase from *Escherichia coli*. *Arch. Biochem. Biophys. 116*, 177–192.

Wray, L.V. & Fisher, S.H. (1988). Cloning and nucleotide sequence of the *Streptomyces coelicolor* gene encoding glutamine synthetase. *Gene 71*, 247–256.